

Supporting information

Expansion counteraction effect assisted vanadate with rich oxygen vacancies as a high cycling stability cathode for aqueous zinc-ion batteries

Xiao-Luan Xie,^b Yi-Fan Li,^b Cheng Wang,^a Da-Wei Gu,^a Lei Wang,^a Qiao Qiao,^b Yang Zou,^b Zhi-Yuan Yao,^{*a} Lin-Jiang Shen,^a Xiao-Ming Ren^{b,c}

^a School of Physical and Mathematical Sciences, Nanjing Tech University, Nanjing 211816, P. R. China

^b State Key Laboratory of Materials-Oriented Chemical Engineering and School of Chemistry and Molecular Engineering, Nanjing Tech University, Nanjing 211816, P. R. China

^c State Key Laboratory of Coordination Chemistry, Nanjing University, Nanjing 210023, P. R. China

Email: zyyao@njtech.edu.cn (ZYY)

Contents

Fig. S1 Crystal structures of **NaNVO** (a) along *a*-axis, (b) along *b*-axis and (c) along *c*-axis.

Fig. S2 XRD pattern of **NaNVO**.

Fig. S3 TG curve of **NaNVO**.

Fig. S4 EPR spectroscopy of **NaVO**.

Fig. S5 (a) SEM image, (b) Na, (c) V and (d) O elemental mapping images of **NaVO**.

Fig. S6 Charging-discharging curves at 0.1 A g^{-1} during the initial five cycles of the **NaVO** cathode.

Fig. S7 Capacitive contributions to total storage for the Zn//**NaVO** battery at different scan rates.

Fig. S8 The tunnel of **NaVO** viewed along the (001), (200) and (-111) plane.

Fig. S9 Zn elemental mapping images of the **NaVO** electrode (a, b) at pristine, (c, d) discharge to 0.1V and (e, f) charge to 1.4 V at first cycle.

Table S1 Rietveld refinement data of **NaVO**.

Table S2 ICP analysis for **NaVO** with the atomic ratio for Na and V.

Table S3 Comparison of the electrochemical performance of **NaVO** and vanadium-based cathode materials for AZIBs.

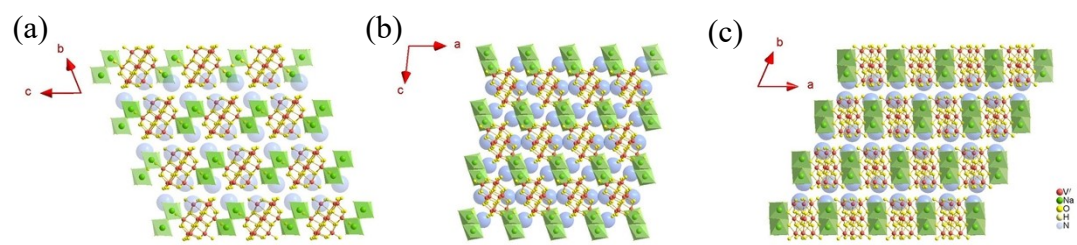


Fig. S1 Crystal structures of NaNVO (a) along *a*-axis, (b) along *b*-axis and (c) along *c*-axis.

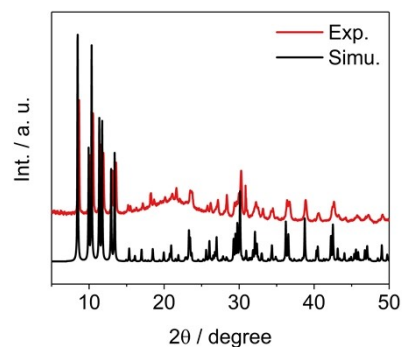


Fig. S2 XRD pattern of NaNVO.

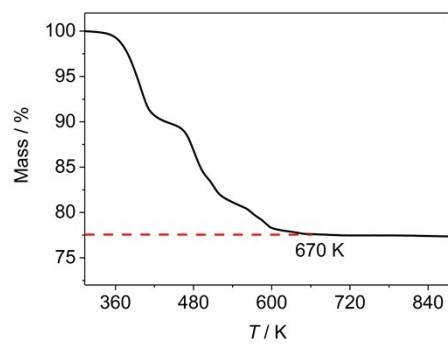


Fig. S3 TG curve of NaNVO.

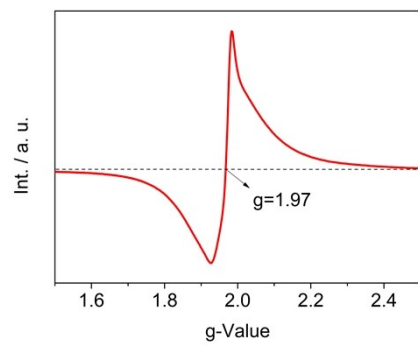


Fig. S4 EPR spectroscopy of **NaVO**.

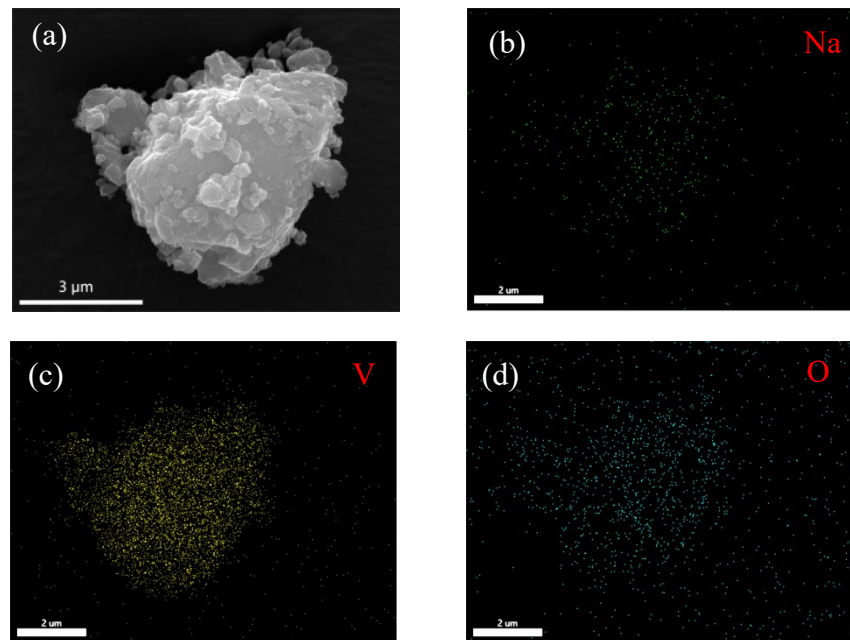


Fig. S5 (a) SEM image, (b) Na, (c) V and (d) O elemental mapping images of **NaVO**.

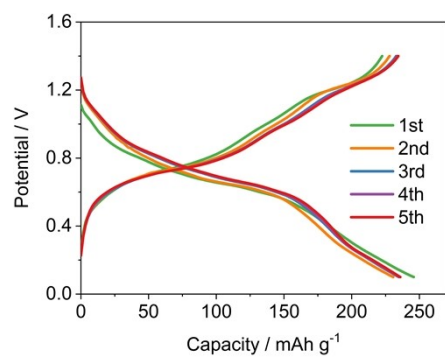


Fig. S6 Charging-discharging curves at 0.1 A g^{-1} during the initial five cycles of the **NaVO** cathode.

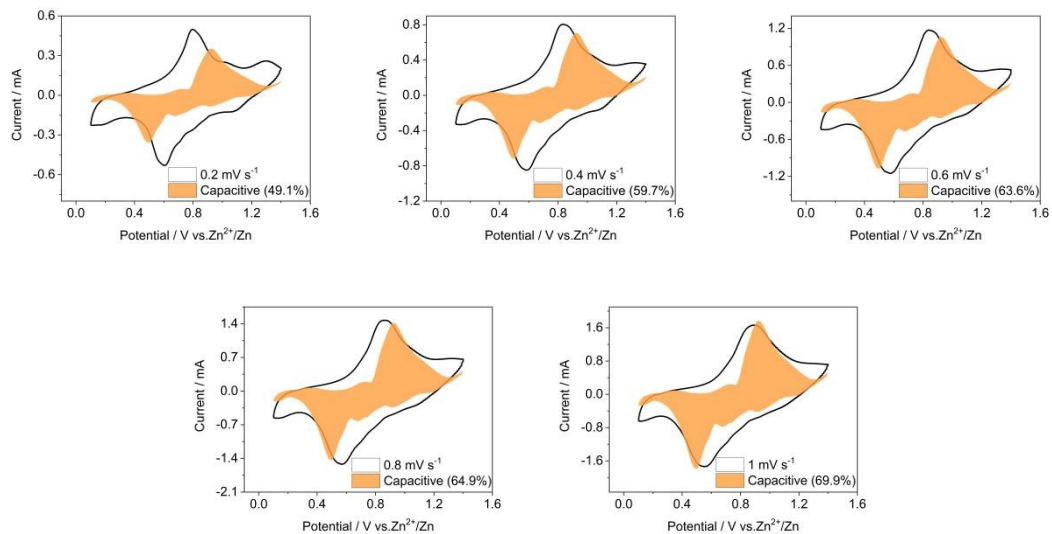


Fig. S7 Capacitive contributions to total storage for the Zn//NaVO battery at different scan rates.

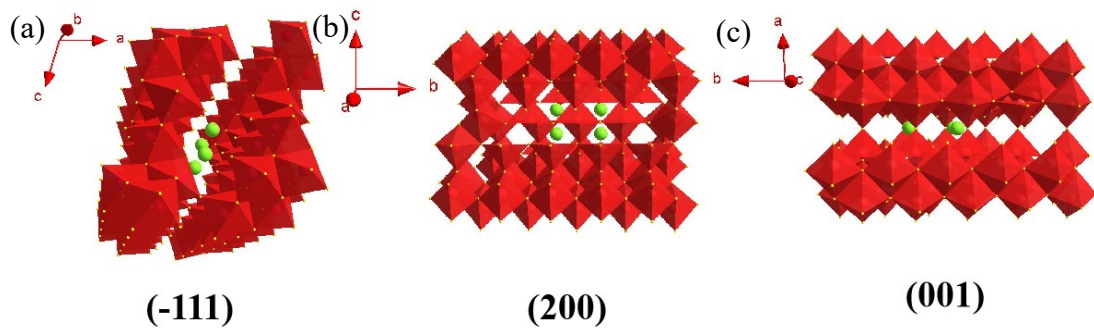


Fig. S8 The tunnel of NaVO viewed along the (a) (001), (b) (200) and (c) (-111) plane.

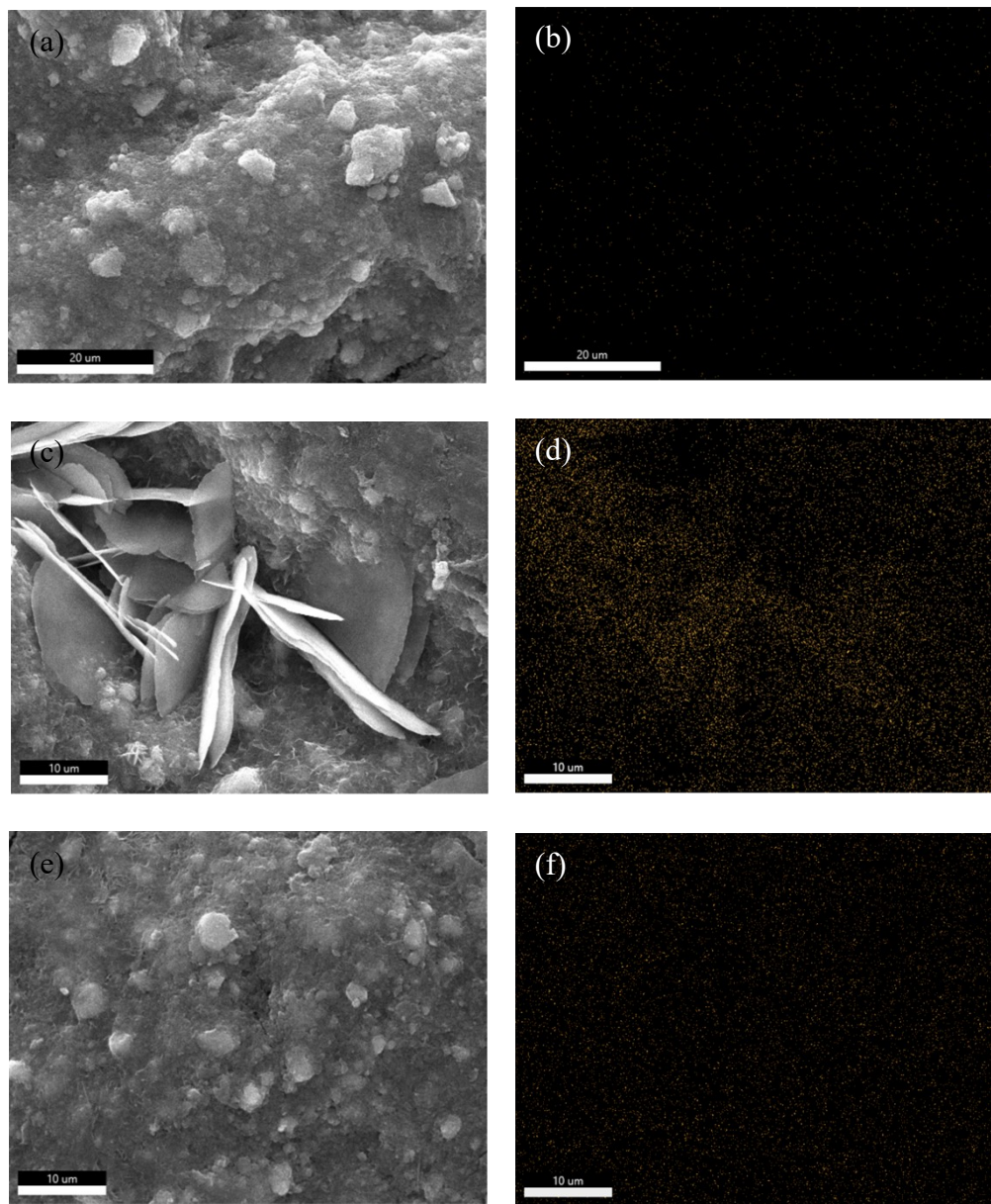


Fig. S9 Zn elemental mapping images of the **NaVO** electrode (a, b) at pristine, (c, d) discharge to 0.1V and (e, f) charge to 1.4 V at first cycle.

Table S1 Rietveld refinement data of **NaVO**.

Rwp = 12.00%		Chi ² : 1.38		
Space group: C 1 2/m 1		$a = 15.45, b = 3.61, c = 10.08 (\text{\AA})$		
		$\alpha = \gamma = 90.00, \beta = 109.56 (\text{^\circ})$		
Atom	X	Y	Z	Occupancy
Na1	-0.00610	0.00000	0.40400	0.34875
V1	0.33652	0.00000	0.10323	0.50000
V2	0.11433	0.00000	0.12256	0.50000
V3	0.28382	0.00000	0.40964	0.50000
O1	0.00000	0.00000	0.00000	0.25000
O2	0.17105	0.00000	-0.03689	0.50000
O3	0.37743	0.00000	-0.08674	0.50000
O4	0.44334	0.00000	0.22874	0.50000
O5	0.25996	0.00000	0.22855	0.50000
O6	0.10292	0.00000	0.27693	0.50000
O7	0.24313	0.00000	0.57003	0.50000
O8	0.39445	0.00000	0.47032	0.50000

Table S2 ICP analysis for **NaVO** with the atomic ratio for Na and V.

Sample	The atomic ratio of Na:V
NaVO	1:4.3

Table S3 Comparison of the electrochemical performance of **NaVO** and vanadium-based cathode materials for AZIBs.

Cathode	Operating conditions (V)	Current density (A g ⁻¹)	Highest capacity (mAh g ⁻¹)	Capacity retention (loss / cycle)	Ref.
Zn ₃ V ₄ (PO ₄) ₆	0.3–1.9	0.11	~104.0	0% / 250	¹
NH ₄ V ₄ O ₁₀	0.4–1.4	0.3	~380.0	26.0% / 50	²
Ni _{0.24} V _{5.76} O ₁₃	0.2–1.4	1.0	~300.0	8.6% / 100	³
Ni _{0.26} V ₂ O ₅ ·1.11H ₂ O	0.3–1.4	0.2	280.7	0% / 40	⁴
CuVO	0.3–1.4	1.0	359.0	26.5% / 50	⁵
Na _{0.56} V ₂ O ₅	0.4–1.5	0.5	196.0	16.0% / 200	⁶
Na _{0.33} V ₂ O ₅	0.2–1.6	0.2	276.6	8.7% / 100	⁷
Na ₆ [V ₁₀ O ₂₈]·nH ₂ O	0.2–1.5	0.3	~150.0	14.4% / 50	⁸
PPy-Na _{1.1} V ₃ O _{7.9}	0.4–1.4	1.0	396.0	0% / 45	⁹
K _{0.52} V ₂ O ₅ ·0.29H ₂ O	0.4–1.4	0.1	300.0	12.0% / 100	¹⁰
LiV ₃ O ₈	0.6–1.2	0.13	~205.0	24.9% / 65	¹¹
LiV ₃ O ₈ @NaV ₃ O ₈	0.3–1.6	0.2	395.5	11.0% / 100	¹²
Zn ₃ V ₃ O ₈ /VO ₂	0.3–1.5	0.3	385.2	7.8% / 200	¹³
Zn _{0.125} V ₂ O ₅ ·0.95H ₂	0.2–1.6	0.2	375.0	~12.0% / 50	¹⁴
O					
NaVO	0.1–1.4	0.1	254.7	9.8% / 150 11.2% / 300 12.7% / 350	This work

References

- [1] D. Zhao, S. Chen, Y. Lai, M. Ding, Y. Cao, Z. Chen, A stable "rocking-chair" zinc-ion battery boosted by low-strain $Zn_3V_4(PO_4)_6$ cathode, *Nano Energy* 100 (2022) 107520.
- [2] Y. Zheng, C. Tian, Y. Wu, L. Li, Y. Tao, L. Liang, G. Yu, J. Sun, S. Wu, F. Wang, Y. Pang, Z. Shen, Z. Pan, H. Chen, J. Wang, Dual-engineering of ammonium vanadate for enhanced aqueous and quasi-solid-state zinc ion batteries, *Energy Storage Mater.* 52 (2022) 664-674.
- [3] Y.-Y. Liu, G.-Q. Yuan, X.-Y. Wang, J.-P. Liu, Q.-Y. Zeng, X.-T. Guo, H. Wang, C.-S. Liu, H. Pang, Tuning electronic structure of ultrathin V_6O_{13} nanobelts via nickel doping for aqueous zinc-ion battery cathodes, *Chem. Eng. J.* 428 (2022) 132538.
- [4] J. Guo, W. Ma, Y. Zheng, H. Chen, Z. Sang, D.a. Yang, Cation pre-intercalation and oxygen vacancies in vanadium oxide for synergistically enhanced high-rate and stability for zinc-ion batteries, *Appl. Surf. Sci.* 612 (2023) 155876.
- [5] Y. Yang, Y. Tang, S. Liang, Z. Wu, G. Fang, X. Cao, C. Wang, T. Lin, A. Pan, J. Zhou, Transition metal ion-preintercalated V_2O_5 as high-performance aqueous zinc-ion battery cathode with broad temperature adaptability, *Nano Energy* 61 (2019) 617-625.
- [6] P. Gao, Q. Ru, H. Yan, S. Cheng, Y. Liu, X. Hou, L. Wei, F. Chi-Chung Ling, A durable $Na_{0.56}V_2O_5$ nanobelt cathode material assisted by hybrid cationic electrolyte for high-performance aqueous zinc-ion batteries, *ChemElectroChem* 7 (2020) 283-288.
- [7] P. He, G. Zhang, X. Liao, M. Yan, X. Xu, Q. An, J. Liu, L. Mai, Sodium ion stabilized vanadium oxide nanowire cathode for high-performance zinc-ion batteries, *Adv. Energy Mater.* 8 (2018) 1702463.
- [8] H. He, F.-C. Pan, X.-W. Liang, Q. Hu, S. Liu, J. Hu, S.C. Jun, D. Lin, Y. Yamauchi, Y. Huo, Unveiling the effect of structural water on Zn-ion storage of polyoxovanadate for high-rate and long-life aqueous zinc ion battery, *Chem. Eng. J.* 462 (2023) 142221.
- [9] S. Islam, S. Lee, S. Lee, M. Hilmy Alfaruqi, B. Sambandam, V. Mathew, J.-Y. Hwang, J. Kim, Triggering the theoretical capacity of $Na_{1.1}V_3O_{7.9}$ nanorod cathode by polypyrrole coating for high-energy zinc-ion batteries, *Chem. Eng. J.* 446 (2022) 137069.
- [10] Q. Li, X. Ye, H. Yu, C. Du, W. Sun, W. Liu, H. Pan, X. Rui, Pre-potassiated hydrated vanadium oxide as cathode for quasi-solid-state zinc-ion battery, *Chin. Chem. Lett.* 33 (2022) 2663-2668.
- [11] M.H. Alfaruqi, V. Mathew, J. Song, S. Kim, S. Islam, D.T. Pham, J. Jo, S. Kim, J.P. Baboo, Z. Xiu, K.-S. Lee, Y.-K. Sun, J. Kim, Electrochemical zinc intercalation in lithium vanadium oxide: A high-capacity zinc-ion battery cathode, *Chem. Mater.* 29 (2017) 1684-1694.
- [12] J. Wang, X. Zhao, J. Kang, X. Wang, H. Yu, C.-F. Du, Q. Yan, Li^+ , Na^+ co-stabilized vanadium oxide nanobelts with a bilayer structure for boosted zinc-ion storage performance, *J. Mater. Chem. A* 10 (2022) 21531-21539.
- [13] L. Yang, J. Jian, S. Wang, S. Wang, A. Abliz, F. Zhao, H. Li, J. Wu, Y. Wang,

Capacity-enhanced and kinetic-expedited zinc-ion storage ability in a $Zn_3V_3O_8/VO_2$ cathode enabled by heterostructural design, Dalton Trans. 51 (2022) 15436-15445.

[14] J.-J. Ye, P.-H. Li, H.-R. Zhang, Z.-Y. Song, T. Fan, W. Zhang, J. Tian, T. Huang, Y. Qian, Z. Hou, N. Shpigel, L.-F. Chen, S.X. Dou, Manipulating oxygen vacancies to spur ion kinetics in V_2O_5 structures for superior aqueous zinc-ion batteries, Adv. Funct. Mater. 33 (2023) 2305659.